Acidic Rate- and Flow-Controlled Dissolution of Uraninite Ores

L. E. EARY, H. L. BARNES, and L. M. CATHLES

A mathematical model is developed to calculate rates of uranium leaching as a function of flow rate and oxidant concentration for acidic solutions. The model is based on a simple plug-flow formulation for the conservation of mass and on experimental rate expressions for the aqueous oxidation of uraninite and pyrite by either ferric ion or hydrogen peroxide. Model calculations of oxidant and dissolved uranium concentrations are generally in good agreement with those measured in column experiments in which synthetic ores consisting of mixtures of uraninite, pyrite, and quartz sand were leached by dilute sulfuric acid solutions (pH = 1.7) that contained ferric ion or hydrogen peroxide as the oxidant. The experimental and modeling results show that uraninite is preferentially leached from pyritic ores by ferric ion solutions, but is less selectively leached by hydrogen peroxide. The calculated and measured rates of uranium leaching for pyritic ores indicate that it is most efficient to use high oxidant concentrations and high flow rates to take advantage of the more rapid reaction rates of uraninite with oxidant compared to reaction rates of pyrite with oxidant. At high flow rates, uranium extraction is maximized throughout a proportionately greater amount of ore before other competing reactions deplete the oxidant concentrations in the leaching solution.

I. INTRODUCTION

IN SITU and dump leaching have become increasingly important methods for extracting uranium from low-grade ores. The basic technology of uranium leaching follows the sequence: (1) application of a leaching solution directly to the uranium ore, (2) dissolution and transport of the dissolved uranium through the ore, and (3) retrieval and recovery of the uranium from solution. Leaching solutions may be either acidic or basic, depending on the host rock mineralogy, but must contain an oxidant such as hydrogen peroxide, ferric ion, dissolved oxygen, or sodium hypochlorite for the efficient extraction of the uranium.[1] Accordingly, the most important factors that control the rate of uranium leaching are the morphological properties of the ore, which control the amount of oxidant that contacts the uranium-bearing minerals, and the rates of dissolution of those uranium minerals by the leaching solutions.

Numerous investigators, including Galichon *et al.*,[2] Sundar,[3] Grant,[4] Tatom,[5] and Goddard and Brosnahan,[6] have conducted column-leaching experiments with natural uranium ores to determine the rates of uranium extraction. However, in these studies unequivocal determinations of the relative importance of the chemical factors, which control the dissolution rates of the uranium minerals, compared to the morphological factors, which control the leachable uranium content in the ore, have been impeded by the complex nature of the reactions occurring between the natural ores and the leaching solutions, and by the lack of sufficient characterization of the ores. In many uranium deposits that have been selected for *in situ* leaching, uraninite (UO_2-U_3O_8) is the most common uranium mineral and may be associated with iron sulfide minerals such as pyrite (FeS_2). The chemical factors that control the rate of uraninite dissolution in acidic solutions have been determined in batch experiments, and rate expressions that describe the UO_2 dissolution rate as a function of the oxidant concentration are given by Eary and Cathles[7] for hydrogen peroxide solutions and by Amell and Langmuir[8] for ferric ion solutions.

This study was conducted to develop a generalized mathematical model that incorporates the rate expressions that are derived from batch experiments to describe the uranium leaching rates in columns as a function of solution chemistry and flow rate. The rate of aqueous oxidation of pyrite is also included in the model, because pyrite oxidation is a competing reaction that depletes the oxidant concentration in the leaching solutions and thereby decreases the rate of uranium leaching. To test the model, we conducted column experiments in which synthetic ores consisting of uraninite, pyrite, and quartz sand were leached by dilute sulfuric acid solutions (pH = 1.7) that contained either hydrogen peroxide or ferric ion as the oxidant. The use of well-characterized synthetic ores allows unambiguous interpretation of the chemical factors controlling the uranium leaching rates in the columns because the morphological properties are greatly simplified, and thus quantitative data on uranium leaching rates are provided that can be compared to model calculations.

II. CHARACTERISTICS OF THE LEACHING MODEL

In the leaching model, the concentration of a reactive fluid species, such as the oxidant, is determined as a function of its reaction rate with oxidizable minerals and the distance traveled in one-dimension along the column axis. We assume that the axial dispersion of the fluid species within the column can be neglected, such that the fluid species are considered to be transported through the column at the same rate as the bulk flow rate. Also, we assume that the void space in the column is completely filled with the leaching solution, and that the porosity in the ore-filled column does not change appreciably because of mineral

L. E. EARY, formerly a Graduate Student with the Department of Geochemistry and Mineralogy, The Pennsylvania State University, is a Research Scientist with Battelle Pacific Northwest Laboratory, Richland, WA 99352. H. L. BARNES is a Professor of Geochemistry and Director, Ore Deposits Research Section, Department of Geosciences, The Pennsylvania State University, University Park, PA 16802. L. M. CATHLES is a Senior Research Geophysicist with Chevron Oil Field Research Company, La Habra, CA 90631.

Manuscript submitted September 20, 1985.

leaching. In all the equations that follow, the subscript i refers to an oxidizing fluid species, such as hydrogen peroxide or ferric ion, and the subscript j refers to the minerals, such as uraninite and pyrite, that are dissolved by reactions with the oxidants. Additionally, the designation "ore" refers to the combined solids plus fluid fractions contained in the column, whereas, for the designation "solids", the fluid fraction is excluded. With these assumptions and definitions, the concentration of an oxidizing species i, as a function of time and distance traveled through the column at a steady flow rate, can be described by the following expression:[9]

$$\rho_w \phi(\partial m_i/\partial t) + \rho_w v(\partial m_i/\partial x) = r_i \qquad [1]$$

In Eq. [1], ρ_w is the density of the fluid in the system in kg/m^3 H_2O (assumed to be equal to the density of water for the leaching solutions), ϕ is the fluid-filled porosity and has units of m^3 H_2O/m^3 ore, m_i is the molal concentration of species i, t is time in seconds, x is the distance traveled in the axial direction in meters, v is the superficial velocity of the leaching fluid and has units of m^3 H_2O/m^2 ore/sec, and r_i is the total rate of reaction for the oxidizing species i in the ore and has units of mol i/m^3 ore/sec. The corresponding rate of dissolution for each mineral j that results from aqueous oxidation by the oxidizing species i is expressed as

$$\rho_s(1 - \phi)(\partial C_j/\partial t) = r_j \qquad [2]$$

where ρ_s is the average density of the solids in the ore and has units of kg solids/m^3 solids, C_j is the molar concentration of the mineral j remaining in the ore and has units of mol j/kg solids, and r_j is the dissolution rate of mineral j in the ore and has units of mol j/m^3 ore/sec.

The total rate of reaction for the oxidizing species i is related to the dissolution rates of up to n minerals as follows:

$$r_i = \sum_{j=1}^{n} \alpha_{i,j} r_j \qquad [3]$$

where $\alpha_{i,j}$ is a stoichiometric coefficient and is equal to the moles of fluid species i consumed per mole of mineral j dissolved.

Expressions that relate the dissolution rates of particular minerals to the concentrations of the oxidizing species are required to use the above equations for describing flow and reaction. In general, rate expressions for mineral dissolution are determined from experimental measurements of concentration change with time in solution-dominated systems, and these rate expressions usually describe the dependence of the dissolution rate on reactant concentrations and on the interfacial surface areas of the dissolving minerals. For example, the dissolution rate for a mineral j that is directly dependent on the concentration of an oxidizing species i is expressed as

$$r_j^d = -k_j^d(A_j/M_w)m_i \qquad [4]$$

where the dissolution rate for the solution-dominated system, r_j^d, has units of mol j/kg H_2O/sec, and k_j^d is a first-order rate constant for the solution-dominated system with units of mol j/mol i/sec. Also, in Eq. [4], the quantity (A_j/M_w) is the ratio of the relative interfacial surface area of mineral j, A_j, to the relative mass of fluid in the system, M_w. These quantities are defined in terms of standard states such that both are dimensionless[10] as follows:

$$A_j = A_j/A^\circ \qquad \text{where } A^\circ = 1 \text{ m}^2 \qquad [5]$$

and

$$M_w = M_w/M_w^\circ \qquad \text{where } M_w^\circ = 1 \text{ kg } H_2O \qquad [6]$$

Rate expressions in the form of Eq. [4] are applicable to solution-dominated systems, but are not consistent with the ore-based rate convention used in the flow and reaction equations (Eqs. [1] and [2]) and must be modified. First, because the ore consists of both a solid and a liquid fraction, we multiply the expression for dissolution rate in Eq. [4] by the fluid density and the ore porosity as follows:

$$r_j = -k_j^d(A_j/M_w)m_i \rho_w \phi \qquad [7]$$

to obtain the dissolution rate for mineral j that is applicable to the fluid-saturated ore. Additionally, the relative interfacial surface area of mineral j is related to its remaining concentration in the ore by

$$A_j = V S_j C_j \rho_s (1 - \phi)/A^\circ \qquad [8]$$

where V is the total volume of ore (m^3 ore) and S_j is the molar surface area of the unreacted mineral j (m^2/mol j). The relative mass of fluid in the ore is given by

$$M_w = V\phi/M_w^\circ \qquad [9]$$

Using the modifications in Eqs. [7], [8], and [9], the dissolution rate of mineral j in the ore is now given by

$$r_j = -k_j' C_j m_i \qquad [10]$$

where

$$k_j' = k_j^d S_j \rho_s (1 - \phi) M_w^\circ/A^\circ \qquad [11]$$

An additional modification is necessary to account for the decrease in the surface area of a dissolving mineral over time. If we assume that all of the dissolving-mineral grains are spherical and have approximately the same radius, then the total surface area of a particular mineral can be related to its remaining concentration in the ore by the following expression that is based on the spherical geometry:

$$S_j = S_j^0 (C_j/C_j^0)^{2/3} \qquad [12]$$

In Eq. [12], S_j^0 and C_j^0 refer to the initial molar surface area and the concentration for mineral j in the ore, respectively. It should be noted that in the development of Eq. [12], surface area effects caused by variable grain sizes or etching of the mineral surfaces are not considered.

From Eqs. [3] and [10], the right side of Eq. [1] is recast in terms of the dissolution rate of the mineral j that is located in the ore as follows:

$$\rho_w \phi(\partial m_i/\partial t) + \rho_w v(\partial m_i/\partial x) = -\left(\sum_{j=1}^{n} \alpha_{i,j} k_j' C_j\right) m_i \qquad [13]$$

Additionally, Eq. [2] is recast in terms of the rate expression given in Eq. [10] as follows:

$$\rho_s(1 - \phi)(\partial C_j/\partial t) = -k_j' C_j m_i \qquad \text{for } j = 1, 2, 3, \ldots, n \qquad [14]$$

Equations [13] and [14] describe the effects of flow on dissolution rates only for rates that are linearly dependent on the concentration of the oxidant. For more complex situations, such as a higher-order rate dependence, other rate

laws can be substituted for Eq. [4] to derive expressions that are analogous to Eqs. [13] and [14].

In order to solve Eqs. [13] and [14] for m_i and C_j as a function of time and distance, it is helpful to rewrite these equations in terms of the dimensionless variables, x′, θ, m_i', and C_j', which are defined as follows:

$$x' = x/L \quad [15]$$

i.e., the fraction of the column length, L, along the column axis,

$$\theta = tv/\phi L \quad [16]$$

i.e., the cumulative number of pore volumes of leaching solution displaced through the ore,

$$m_i' = m_i/m_i^0 \quad [17]$$

i.e., the mole proportion of the initial concentration of species i remaining in the leaching solution, and

$$C_j' = C_j/C_j^0 \quad [18]$$

i.e., the mole proportion of the initial concentration of mineral j remaining in the ore. By rewriting Eqs. [13] and [14] in terms of the dimensionless variables given in Eqs. [15] to [18] we obtain the following expressions:

$$(\partial m_i'/\partial\theta) + (\partial m_i'/\partial x') = -\left(\sum_{j=1}^{n} D_j C_j'\right) m_i' \quad [19]$$

and

$$(\partial C_j'/\partial\theta) = -D_j B_i C_j' m_i' \quad \text{for } j = 1, 2, 3, \ldots, n \quad [20]$$

In Eqs. [19] and [20], D_j is the Damokohler number for mineral j and is defined as the ratio of the rate of dissolution of mineral j to the rate of flow through the ore as follows:[7]

$$D_j = (\alpha_{i,j} k_j' C_j^0 L)/(v\rho_w) \quad [21]$$

The quantity B_j in Eq. [20] is referred to as the oxidant capacity number for mineral j, and is defined in the following expression as the ratio of the amount of the oxidizing species i present in the pore volume to the amount of i required to dissolve all of the mineral j present in a unit volume of ore:

$$B_i = (\phi m_i^0 \rho_w)/(\alpha_{i,j} \rho_s (1 - \phi) C_j^0) \quad [22]$$

The analytical functions for flow and reaction given in Eqs. [19] and [20] were solved by a finite-difference method that involved a Newton-Raphson iterative technique for the following initial conditions that are relevant to the column-leaching experiments:

$$m_i' = 1.0 \quad \text{at } x' = 0.0 \quad [23]$$

and

$$C_j' = 1.0 \quad \text{at } \theta \leq x' \quad [24]$$

Solutions to these modeling equations are compared to the results obtained in column-leaching experiments in Section V.

III. REACTIONS AND RATE EXPRESSIONS

The reactions and rate expressions that were used to model the column-leaching experiments are listed in Table I. For simplicity, the reactions in Table I are written in general form in which the ion-pairing of the aqueous species is neglected. Additionally, sulfate species are expected to be the dominant sulfur oxidation products that result from the aqueous oxidation of pyrite in acidic solutions.[14,15]

Although some generalized rate expressions for reactions [1] and [2] in Table I were available in the literature, a number of preliminary column experiments were conducted to check the forms of these rate expressions and to obtain rate constants for the specific conditions of the experiments.[11] For reaction [1] in Table I, Amell and Langmuir[8] give a rate constant, $k = 10^{-3.8}$ mol UO_2/mol Fe^{3+}/sec. A nearly equivalent $k = 10^{-4.0}$ mol UO_2/mol Fe^{3+}/sec was obtained from column-leaching experiments by Eary[11] and is used here. The rate expression for reaction [2] in Table I was determined from four column experiments in which mixtures of pyrite and quartz sand were leached by ferric ion solutions at a pH of 1.7. Plots of the logarithm of ferric ion concentration remaining in solution *vs* the displacement time, t_d, which is given by

$$t_d = \phi x/v \quad [25]$$

yielded linear relationships indicating that the rate of reaction [2] in Table I was linearly dependent on the concentration of ferric ion remaining in solution. This first-order dependence is similar to the results reported by Wiersma and Rimstidt[12] and Singer and Stumm[13] for the aqueous oxidation of pyrite by ferric ion in acidic solutions. The rate expressions for reactions [3] and [4] in Table I are taken directly from Eary and Cathles[7] and McKibben,[14] respectively.

IV. EXPERIMENTS

A. *Materials*

The synthetic ores used in the column experiments consisted of mixtures of medium- to fine-grained quartz sand, granulated pyrite, and granulated uraninite. All minerals

Table I. Summary of Dissolution Reactions and Rate Expressions Used in the Model Calculations

Reaction	$-r_j^d =$	Reference
[1] $UO_2 + 2Fe^{3+} \rightarrow UO_2^{2+} + 2Fe^{2+}$	$10^{-4.0}(A/M_w)(m\ Fe^{3+})$	Eary,[11] Amell and Langmuir[8]
[2] $FeS_2 + 14Fe^{3+} + 8H_2O \rightarrow 15Fe^{2+} + 2HSO_4^- + 14H^+$	$10^{-6.2}(A/M_w)(m\ Fe^{3+})$	Eary,[11] Wiersma and Rimstidt,[12] Singer and Stumm[13]
[3] $UO_2 + H_2O_2 + 2H^+ \rightarrow UO_2^{2+} + 2H_2O$	$10^{-4.0}(A/M_w)(m\ H_2O_2)$*	Eary and Cathles[7]
[4] $FeS_2 + 7.5H_2O_2 + H^+ \rightarrow Fe^{3+} + 2HSO_4^- + 7H_2O$	$10^{-5.5}(A/M_w)(m\ H_2O_2)$	McKibben[14]

*Rate constant is modified for total sulfate concentration as follows: $k = 10^{-4.0} \exp(-m\ SO_4^{2-}/10^{-2.38}) + 10^{-4.27}$.

were identified from powder X-ray diffraction patterns, and were prepared by various procedures before being combined to create the synthetic ores. The quartz sand was prepared by leaching for 10 to 16 hours in a concentrated acid solution that contained by volume 90 pct concentrated HCl + 9 pct concentrated HNO_3 + 1 pct 8.8 *m* H_2O_2 to remove iron oxide coatings and organic material. The pyrite, which was obtained as 1- to 3-cm crystals, was crushed and sieved to separate the 0.105- to 0.25-mm-size fraction. This fraction was leached in a 0.1 *m* HNO_3 + 0.1 *m* HCl solution for 15 to 20 minutes, and was then repeatedly rinsed in deionized water. Also, immediately before the prepared pyrite grains were added to a synthetic ore mixture, they were preleached in 0.1 *m* HCl solutions for approximately five minutes to remove any surface films of iron oxide. The uraninite was obtained in the form of sintered pellets. Analyses of these pellets by powder X-ray diffraction and calculation of the unit cell dimensions[16] indicated that they consisted of stoichiometric UO_2. These pellets were crushed and sieved to obtain the 0.053- to 0.074-mm-size fraction, and were then placed in a rocking autoclave with a 0.5 *m* $NaHCO_3$ solution and a methane atmosphere. The autoclave was heated to 300 °C for 12 to 14 days and was then slowly cooled over three days to room temperature to anneal the surfaces of the UO_2 grains. The annealed grains were determined from X-ray diffraction patterns to still be stoichiometric UO_2. The specific surface areas of the prepared pyrite and UO_2 grains were measured by the BET gas adsorption method using argon as the adsorbate gas, and were determined to be 0.024 m^2/g and 0.189 m^2/g for the pyrite and the UO_2, respectively, which give molar surface areas of 2.88 m^2/mol pyrite and 51.03 m^2/mol UO_2.

B. *Procedure*

The synthetic ore mixtures were made by thoroughly dispersing appropriate weights of the prepared UO_2 and pyrite grains in a measured weight of quartz sand. The columns consisted of polyvinylchloride tubes with inside diameters of 2.35 cm and lengths ranging from 88 to 100 cm. The synthetic ores were packed into the columns by tamping with a steel rod, and a 100-cm long column contained about 0.720 kg of ore. The porosities of the packed columns were consistently determined to be equal to 0.37 (±0.02) based on the column dimensions, ore weight, and average mineral densities. Solution samples were collected at the effluent end of a column and through three stainless steel capillary lines, which were located at distances of ¼, ½, and ¾ of the total column length from the injection end (Figure 1). The

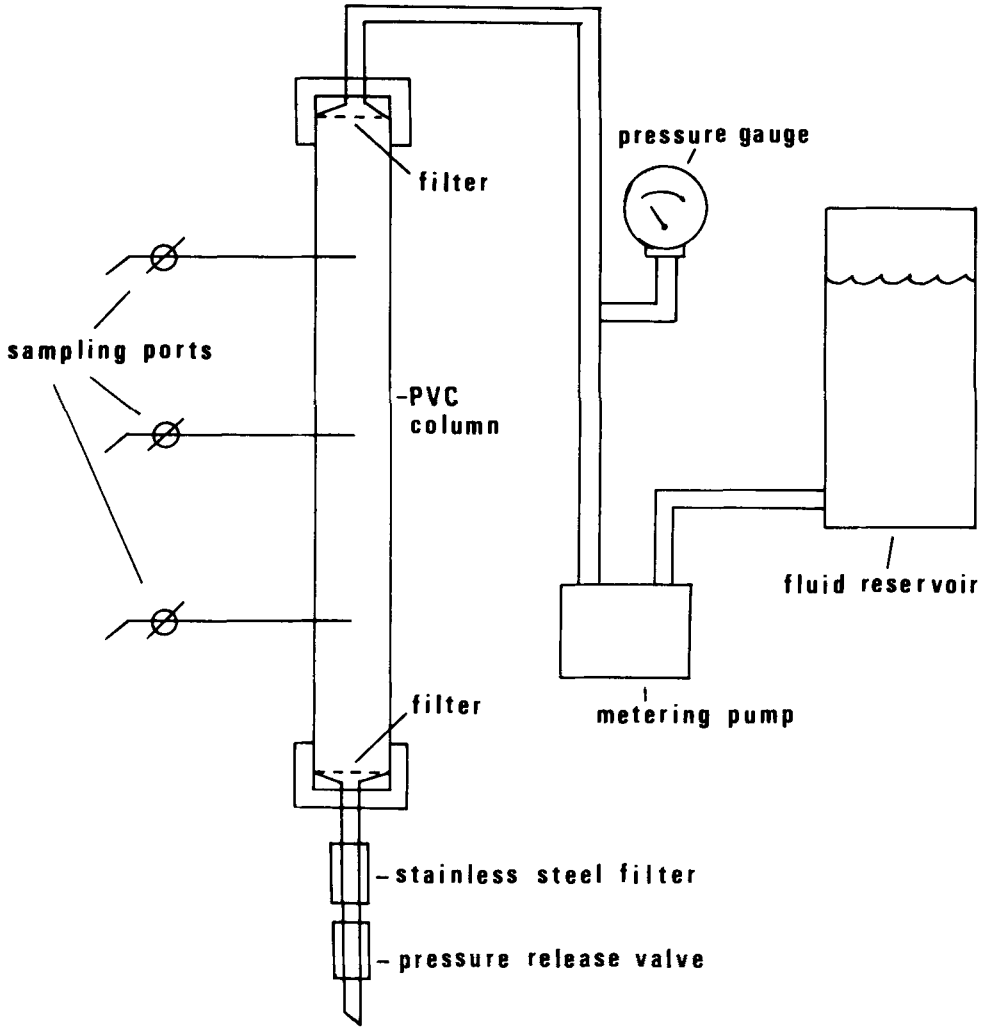

Fig. 1—Apparatus for the column experiments.

sampling ports located on the sides of the columns permitted the determination of the oxidant and dissolved uranium concentrations in the pore fluids as a function of distance from the injection end of the column.

Each of the column-leaching experiments was started by injecting distilled water into the ore-filled column with a metering pump to displace the air and to bring the column up to a hydrostatic pressure of 50 (±5) psi. This pressure was maintained during leaching by a pressure release valve located at the discharge end of the column. After the air was purged from the columns, the reservoir of leaching solution was connected to the metering pump to begin the actual leaching of the ore mixtures. The temperature was maintained at 25 (±3) °C by pumping water from a constant temperature bath through copper tubing that was wrapped tightly around the column.

The oxidant source for the leaching solutions was either a reagent-grade ferric sulfate solid or an 8.8 *m* H_2O_2 stock solution. One of these oxidants, along with an appropriate amount of sulfuric acid, were mixed in distilled water to create leaching solutions with a pH of 1.7. The concentration of H_2O_2 in the reservoir solutions was periodically measured, but no decomposition was evident over the duration of the column-leaching experiments.

C. *Analytical*

Solution samples of 3 to 5 ml were simultaneously withdrawn through each of the sampling ports and were also collected at the effluent end of the column. The pH of these samples was measured with a glass combination pH-reference electrode and was consistently determined to be 1.70 (±0.10). The concentrations of dissolved uranium, ferrous and total iron, and H_2O_2 were determined by colorimetric methods 30 to 60 minutes after sampling. The uranium concentrations were determined using the dibenzoylmethane chromagen after extraction from acidic solutions with tributylphosphate.[17] The concentrations of ferrous and total iron were determined using the ferrous-orthophenanthroline chromagen,[18,19] and the ferric concentrations were determined by difference. The concentrations of H_2O_2 were determined using a titanium sulfate chromagen.[20]

V. RESULTS AND DISCUSSION

A. *Ferric Ion as the Oxidant*

Typical concentration profiles for ferric ion and UO_2 as a function of distance from the injection ends of the columns are shown in Figures 2 and 3 for columns that initially contained 0.5 wt pct UO_2 + 99.5 wt pct quartz sand. For both Figures 2 and 3, the initial concentration of ferric ion in the leaching solutions was the same, but the flow rate for the experiment depicted in Figure 3 was three times that indicated for Figure 2. The symbols in Figures 2(a) and 3(a) show the measured concentrations of ferric ion in solution samples that were simultaneously collected through the three sampling ports and at the effluent ends of the columns (see Figure 1). The numbers enclosed within the symbols indicate the cumulative number of pore volumes, θ, of leaching solution that had been displaced through the columns at the time of sampling (see Eq. [16]). At a constant

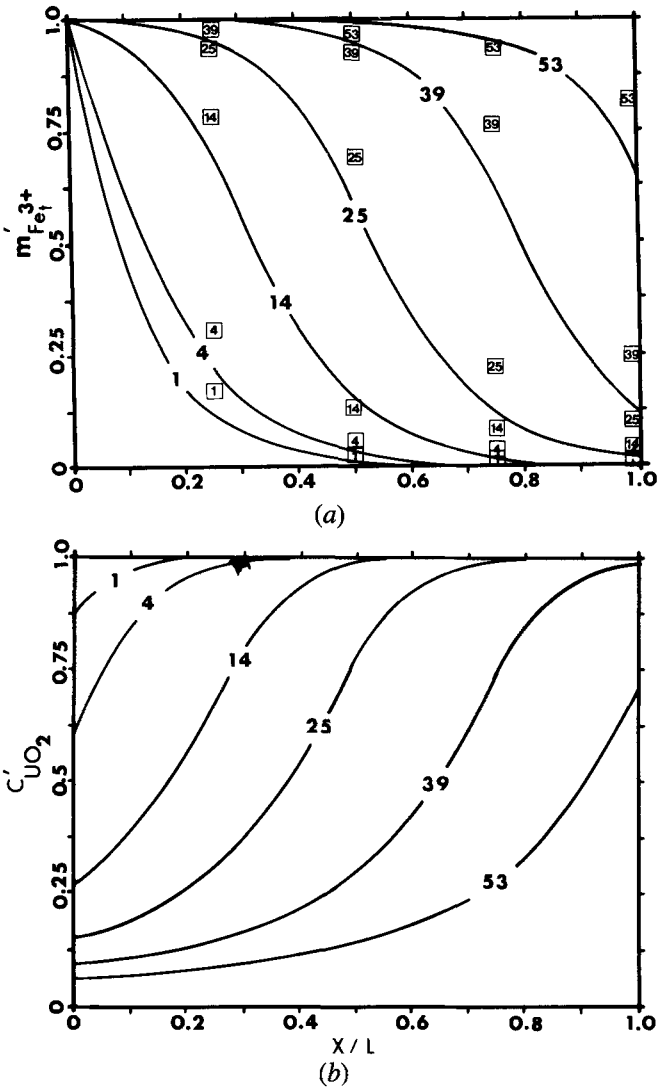

Fig. 2—Typical changes in the proportional concentrations of (*a*) ferric ion and (*b*) UO_2 as a function of the fractional distance from the injection end of the column and the cumulative pore volumes of leaching solution. This column initially contained 0.5 wt pct UO_2 + 99.5 wt pct quartz sand, and was leached at v = $10^{-4.34}$ m^3 H_2O/m^2 ore/sec with a $10^{-2.47}$ *m* ferric ion solution (pH = 1.7).

flow rate, the cumulative pore volumes displaced is a measure of time such that the measured oxidant concentrations in the columns can be compared to the solid curves, which represent model calculations of the remaining ferric ion concentration, to determine the rate of leaching as a function of distance after a specific period of time. For the specific pore volumes at which solution samples were collected, comparisons of the measured ferric ion concentrations to the calculated curves indicate reasonably good agreement for both flow rates, showing that the leaching rates calculated with the model accurately portray the rates of oxidant loss caused by reaction with the UO_2 in these columns. The concentrations of UO_2 remaining in the columns were not measured.

The profiles in Figures 2 and 3 also show the progress of UO_2 leaching as a function of the cumulative number of pore volumes of leaching solution that were displaced through the ore-filled columns. For the initial pore volumes, the rate of UO_2 dissolution is most rapid in the upstream portions of the

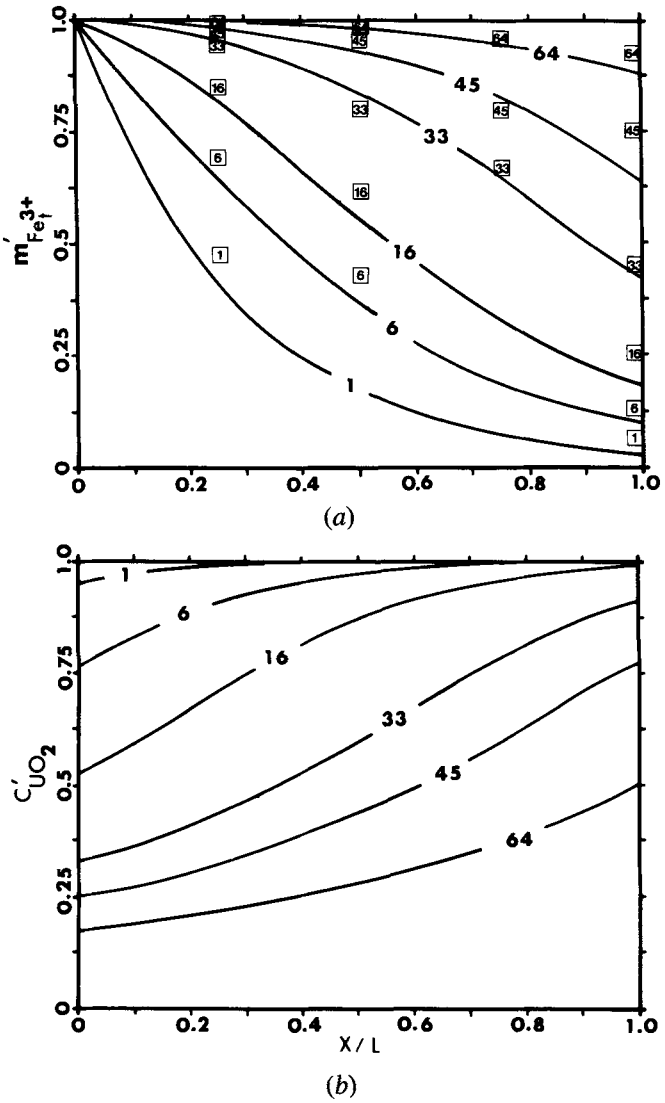

Fig. 3—Typical changes in the proportional concentrations of (*a*) ferric ion and (*b*) UO_2 as a function of the fractional distance from the injection end of the column and the cumulative pore volumes of leaching solution. This column initially contained 0.5 wt pct UO_2 + 99.5 wt pct quartz sand, and was leached at v = $10^{-3.86}$ m^3 H_2O/m^2 ore/sec with a $10^{-2.47}$ *m* ferric ion solution (pH = 1.7).

columns where both the remaining ferric ion and UO_2 concentrations are highest, and as a result, very little of the original ferric ion content of the injected solution reaches the end of the column (Figures 2(a) and 3(a)). After continued leaching, the UO_2 content is depleted in the upstream sections of the columns, and the region where the most rapid leaching takes place, as indicated by the steepest slopes of the concentrations profiles, moves downstream in the direction of the higher residual UO_2 concentrations.

The formation of a fast leaching or reaction zone is dependent on the Damokohler number, the ratio of the reaction rate to the rate of fluid flow (see Eq. [21]). Systems with high Damokohler numbers show steep reaction fronts that indicate rapid changes in reactant concentrations over short distances, whereas systems with relatively lower Damokohler numbers show more shallow fronts.[9] The effect of decreasing the Damokohler number by increasing the flow rate can be seen by comparing the concentration profiles for ferric ion and UO_2 in Figure 2 with those in Figure 3. The profiles in Figure 3 show measured and calculated concentrations for UO_2 leaching by a ferric ion solution with the same initial composition as for Figure 2, but at a flow rate three times as fast. The reaction fronts in Figure 3 are not as steep with respect to distance as those in Figure 2, indicating that dissolution of the UO_2 takes place more evenly throughout the entire length of the column at the higher flow rate, rather than primarily within a short segment.

The model was also used to calculate effluent uranium concentrations as a function of the cumulative pore volumes of leaching solution displaced through the columns. The calculated concentrations are shown in Figure 4 as the solid curves and are compared to the measured uranium concentrations. Figure 4(a) shows the effects of flow rate on UO_2 leaching for the same initial ferric ion concentration, and Figure 4(b) shows the effects of different ferric ion concentrations for the same flow rate. An increase in the ferric ion concentration in the leaching solution or a decrease in the flow rate result in proportionately greater rates of uranium

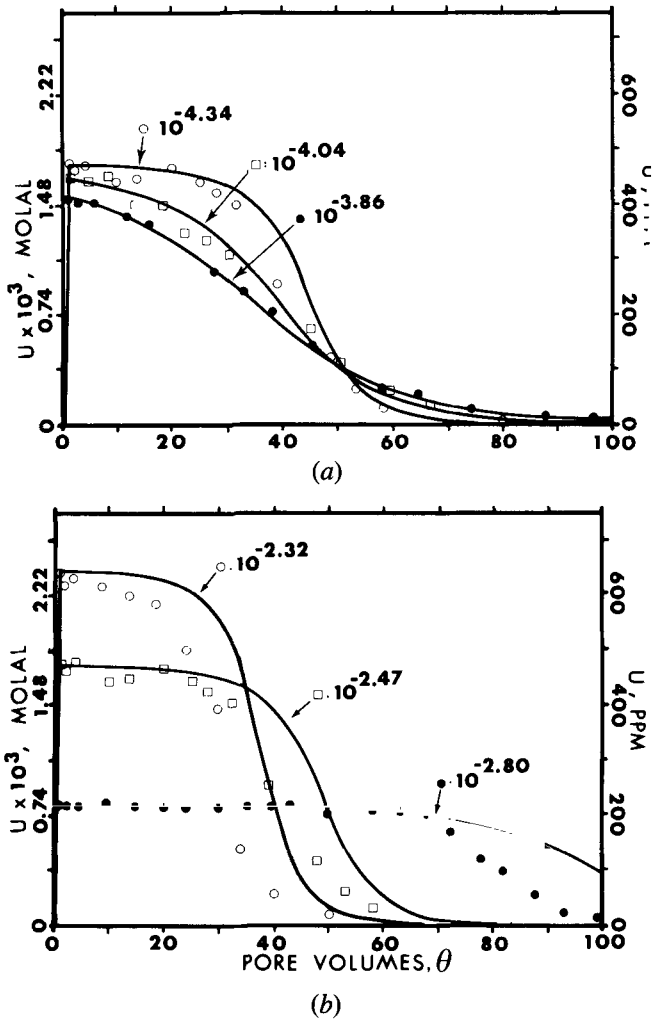

Fig. 4—Rates of uranium leaching, as indicated by the dissolved uranium concentrations in column effluents (*a*) for the three indicated flow rates by $10^{-2.47}$ *m* ferric ion solutions (pH = 1.7), and in (*b*) for the three indicated concentrations of ferric ion for the same flow rate of $10^{-4.34}$ m^3 H_2O/m^2 ore/sec. These columns initially contained 0.5 wt pct UO_2 + 99.5 wt pct quartz sand.

leaching because the rate of UO_2 dissolution is linearly dependent on the concentration of ferric ion (Table I).

The addition of pyrite to the synthetic UO_2 ores resulted in only a small decrease in the rate of UO_2 dissolution as shown by the uranium concentrations that were determined in column effluents during the leaching of ores that contained 0.5 wt pct UO_2 + 3.0 wt pct pyrite + 96.5 wt pct quartz sand (Figure 5). The small decrease indicates that the rate of UO_2 leaching is not sensitive to the pyrite content because the rate of aqueous oxidation of the pyrite by the ferric ion is relatively slow compared to the rate of UO_2 dissolution. The large difference in reaction rates results in the preferential leaching of the UO_2, indicating that the reactions which compete for oxidant can be considered as a system of parallel reactions. In such a system, the fastest reaction controls the overall leaching rate.[21] As a result, uranium ores must have a pyrite content that is significantly higher than the UO_2 content before the rate of pyrite oxidation is increased to the extent that it effectively reduces the amount of ferric ion that is available to oxidize the UO_2.

The model calculations of dissolved uranium concentrations in effluent solutions are generally in good agreement with the experimental measurements (Figures 4 and 5), indicating that the rate expression for the oxidation of UO_2 by ferric ion in Table I accurately describes the leaching rates in our column experiments.

B. *Hydrogen Peroxide as the Oxidant*

Rates of uranium leaching were also measured in columns that contained 0.5 wt pct UO_2 + 99.5 wt pct quartz sand as a function of the flow rate and the H_2O_2 concentration. The calculated profiles for the H_2O_2 concentrations as a function of the distance from the injection end were in very good agreement with the measured concentrations. The shapes of these concentration profiles were similar to those obtained for the ferric ion experiments (Figures 2 and 3), but showed that the UO_2 was more rapidly leached by the concentrations of H_2O_2 used in these experiments ($10^{-2.15}$ to $10^{-2.80}$ $m_{H_2O_2}$).

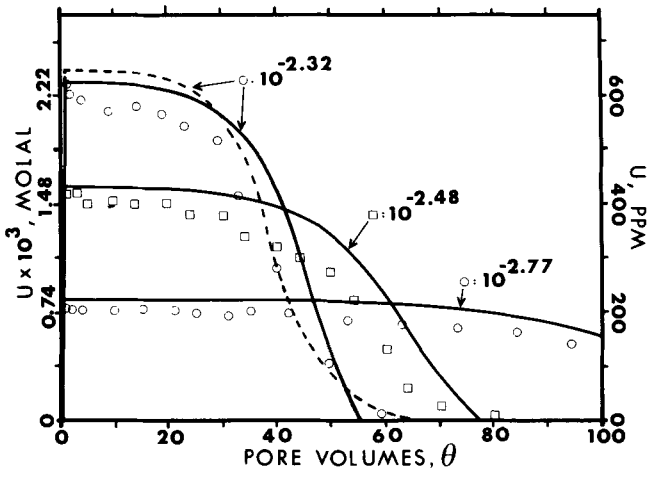

Fig. 5—Rates of uranium leaching, as indicated by the dissolved uranium concentrations in column effluents for the three indicated concentrations of ferric ion (pH = 1.7) and a flow rate of $10^{-4.34}$ m^3 H_2O/m^2 ore/sec. These columns initially contained 0.5 wt pct UO_2 + 3.0 wt pct pyrite + 96.5 wt pct quartz sand. For comparison, the dashed curve indicates the rate of uranium leaching calculated for a column that does not contain pyrite.

This more rapid rate of leaching is also indicated by the measured and calculated uranium concentrations in column effluents that are shown in Figure 6 as a function of the cumulative number of pore volumes of leaching solution that were displaced through the columns. The uranium concentrations in Figure 6(a) show that a decrease in the flow rate causes a proportional increase in the uranium concentration in column effluents. An increase in the H_2O_2 concentration also results in a proportionate increase in the rate of uranium leaching (Figure 6(b)), as would be expected from the first-order dependence of the UO_2 dissolution rate on H_2O_2 concentration (reaction [3] in Table I). The good agreement between the measured and the calculated uranium concentrations shows that the rate expression for UO_2 dissolution in H_2O_2 solution given in Table I is descriptive of the leaching rates in the columns.

Three more column-leaching experiments were conducted with H_2O_2 solutions to measure the effect of pyrite on the rate of uranium leaching. These columns contained 3.0 wt pct pyrite + 0.5 wt pct UO_2 + 96.5 wt pct quartz sand, and the measured and calculated uranium concen-

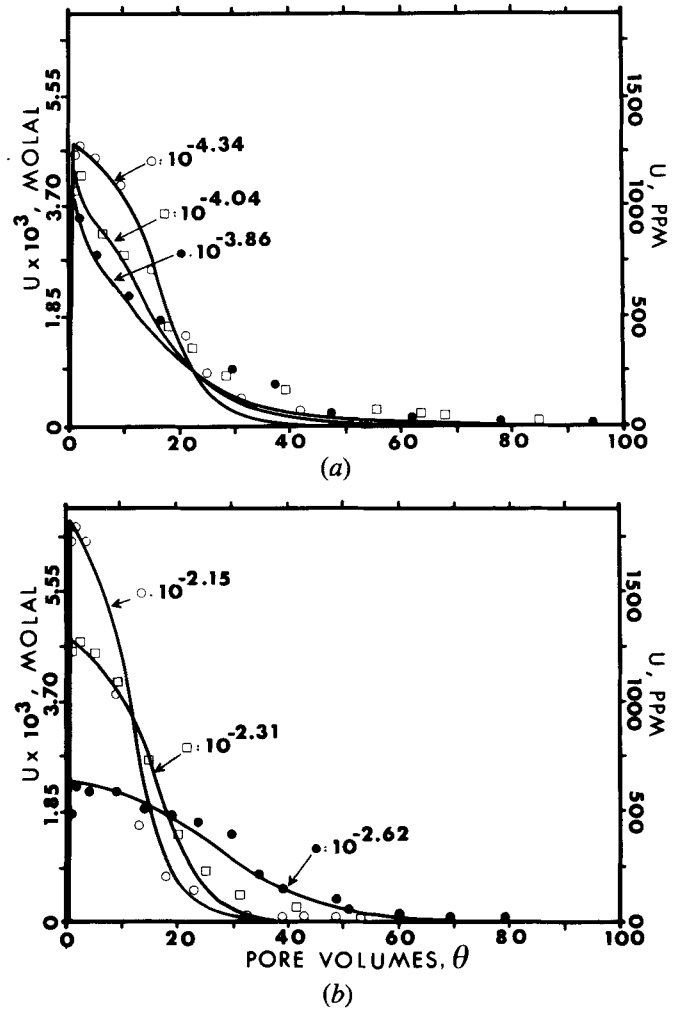

Fig. 6—Rates of uranium leaching, as indicated by the dissolved uranium concentrations in column effluents (*a*) for the three indicated flow rates for a $10^{-2.32}$ *m* H_2O_2 solution (pH = 1.7), and in (*b*) for the three indicated concentrations of H_2O_2 for the same flow rate of $10^{-4.34}$ m^3 H_2O/m^2 ore/sec. These columns initially contained 0.5 wt pct UO_2 + 99.5 wt pct quartz sand.

trations in column effluents for three initial H_2O_2 concentrations are shown in Figure 7. The rate of uranium leaching was found to be significantly decreased by the addition of the pyrite compared to the pyrite-free ores (Figure 6(b)). This decrease occurs because the rate of pyrite oxidation by the H_2O_2 is rapid enough to cause a decrease in the amount of H_2O_2 available to oxidize the UO_2.

The uranium concentrations that were calculated with the model were consistently higher than those measured in column effluents (Figure 7). This discrepancy may have been caused by the loss of some of the H_2O_2 by homogeneous decomposition reactions that can be catalyzed by the free ferric ion and which were not included in the model calculations. Consequently, we used the rate expression of Eary[22] for the ferric ion-catalyzed decomposition of H_2O_2, given by

$$-(dm_{H_2O_2}/dt) = -10^{-2.37}(sec^{-1})\,(m_{H_2O_2})\,(m_{Fe^{3+}})\,(m_{H^+})^{-1} \quad [26]$$

to calculate the maximum amount of H_2O_2 that might be lost by decomposition. The highest concentration of free ferric ion in the acidic sulfate solutions was calculated to be approximately $10^{-4.6}$ *m*. Using this value for the free ferric ion, the highest H_2O_2 concentration of $10^{-2.14}$, a pH of 1.7, and a maximum residence time of 2.5 hours, we calculate that at most about 5 pct of the original H_2O_2 in the leaching solutions could be consumed in ferric ion-catalyzed decomposition reactions. Clearly, other factors are needed to explain the discrepancies between the calculated and the measured uranium concentrations. We expect that a combination of factors, including decomposition reactions and inaccuracies in the rate expression for the aqueous oxidation of pyrite by H_2O_2, contribute to the observed differences between the measured and calculated results shown in Figure 7. For the mineral concentrations used in these experiments, the model is sensitive to even small inaccuracies in the rate expressions because the pyrite contents were great enough to cause the rate of aqueous pyrite oxidation in the H_2O_2 solutions to be similar in magnitude to the rate of aqueous UO_2 oxidation. For systems in which one reaction rate dominates, we would expect the differences between calculated and measured rates to be less, as in the case of ferric ion leaching of pyrite-containing uraninite ores. Nevertheless, these experiments on the H_2O_2 leaching of pyrite and UO_2 indicate that this oxidant is rapidly exhausted, and show that UO_2 is less selectively leached from pyritic ores by H_2O_2 than by ferric ion.

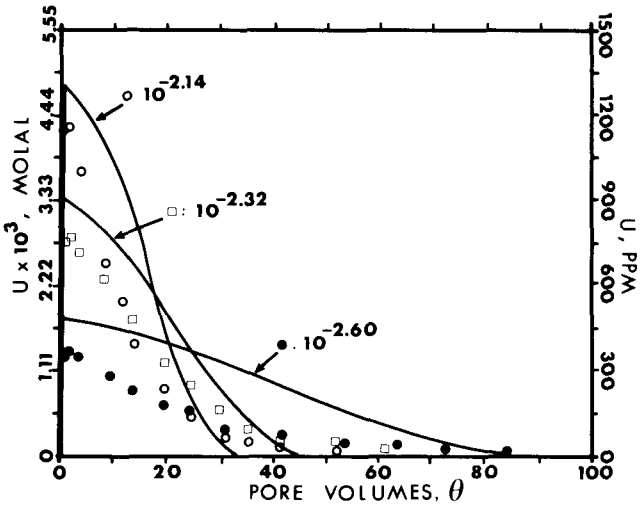

Fig. 7—Rates of uranium leaching, as indicated by the dissolved uranium concentrations in column effluents, from columns that initially contained 0.5 wt pct UO_2 + 3.0 wt pct pyrite + 96.5 wt pct quartz sand for the three indicated concentrations of H_2O_2 (pH = 1.7) and a flow rate of $10^{-4.34}$ m^3 H_2O/m^2 ore/sec.

VI. CONCLUSIONS

The rates of UO_2 leaching that are calculated with the modeling equations presented here are generally in good agreement with the rates observed in the column-leaching experiments. This result indicates that the modeling approach used here can be used to incorporate empirical rate expressions to describe the effects of solution composition and flow rate on the progress of dissolution reactions in column-leaching experiment given sufficient characterization of the reacting solids.

Additionally, the results of the column-leaching experiments and the model calculations can be used to make some broad generalizations about the effect of pyrite on the rate of UO_2 leaching. In acidic solutions, ferric ion more selectively oxidizes UO_2 in pyritic ores compared to H_2O_2. Although the degree of preferential leaching is strongly dependent on the relative amounts of pyrite and UO_2 in the ore, the ratio of the dissolution rate to the flow rate (*i.e.*, the Damokohler number) can be expected to be significantly higher for UO_2 than for pyrite in ferric ion leaching solutions. However, the Damokohler number for UO_2 dissolution in H_2O_2 solutions may be only slightly higher than for pyrite, depending on the pyrite content of the ore.

In experimental columns and in the field, a difference in the dissolution rates will result in a separation of the reaction front for the aqueous oxidation of the uraninite from the front resulting from the aqueous oxidation of the pyrite. Both reaction fronts will migrate in the direction of flow and may become more distinctly separated after the depletion of the uraninite from the regions nearest the point of injection of the leaching solution. Based on this concept of moving reaction fronts, the progress of uranium leaching in a pyritic ore can be described in terms of three overlapping stages. (1) In the initial stage of leaching, a zone of rapid uranium leaching will occur near the point of injection of the oxidant into the ore. Uranium extraction may be rapid within this zone as the uraninite is selectively leached, although some dissolved uranium may be precipitated in downstream areas after the exhaustion of the oxidant. (2) After the depletion of the uranium in the region nearest the injection point, the oxidant must travel a greater distance through ore that is depleted of uraninite but is not depleted of pyrite. As a result of the continued oxidation of the pyrite, the amount of oxidant available for dissolving the uraninite that is located in downstream regions is reduced, resulting in a net decrease in the rate of uranium extraction. (3) In the final stage of leaching, the zone of undepleted uraninite may be so far from the injection point that the majority of the oxidant is consumed in upstream regions by the oxidation of pyrite. By this time, the leaching solution no longer efficiently dissolves the accessible uraninite and the rate of uranium extraction is likely to remain very low.

The above description of uranium leaching in terms of moving reaction fronts that are caused by variable rates of the reactions that compete for oxidant is similar to that given by Goddard and Brosnahan[6] for the leaching of pyritic uranium ores by dissolved oxygen in basic solutions. It is also consistent with the conclusions reached by Tsui,[23] who investigated the mineralogical changes in natural ores that were leached by oxidizing solutions. We suggest, in agreement with Goddard and Brosnahan,[6] that it is advantageous to use high oxidant concentrations and high flow rates to prolong the period of rapid and preferential leaching of UO_2 that occurs during the first stages of leaching.

NOMENCLATURE

- A Interfacial surface area (m^2).
- A Relative interfacial surface area (= A/A° where $A^\circ = 1\ m^2$).
- $B_{i,j}$ Oxidant capacity number (see Eq. [22], dimensionless).
- C_j Molar concentration of mineral j in the ore (mol j/kg solids).
- C_j' Proportion of mineral j remaining in the ore (= C_j/C_j^0).
- D_j Damokohler number for mineral j (see Eq. [21], dimensionless).
- k_j^d First order rate constant for solution-dominated systems (mol j/mol i/sec).
- k_j' Modified first order rate constant ((kg solid · kg H_2O)/(m^3 ore · mol i · sec)).
- kg Kilogram.
- L Column length (m).
- m Meter.
- m_i Molal concentration of i (mol i/kg H_2O).
- m_i' Proportion of i remaining in solution (= m_i/m_i^0).
- M_w Mass of fluid (kg H_2O).
- M_w Relative mass of fluid (= M_w/M_w° where M_w° 1 kg H_2O).
- r Reaction rate in the ore (mol/m^3 ore/sec).
- r_j^d Dissolution rate for solution-dominated systems (mol j/kg H_2O/sec).
- S_j Molar surface area of mineral j (m^2/mol j).
- t Time (sec).
- t_d Displacement time (= $\phi x/v$, sec).
- v Superficial flow velocity (m^3 H_2O/m^2 ore/sec).
- V Total volume of ore (m^3 ore).
- x' Fraction of column length (= x/L).
- $\alpha_{i,j}$ Stoichiometric coefficient (mol i/mol j).
- ρ_s Density of solids in the ore (kg solids/m^3 solids).
- ρ_w Density of the leaching fluid (= 999.0 kg H_2O/m^3 H_2O at 25 °C).
- ϕ Fluid-filled porosity (m^3 H_2O/m^3 ore).
- θ Cumulative pore volumes (= $tv/\phi L$, dimensionless).
- fluid Refers to the water-based leaching solution.
- ore Refers to the combined fluid plus solids fractions in the column.
- solids Refers to only the solid fraction in the column.

Subscripts

- i Refers to the oxidizing species, *i.e.*, ferric ion or H_2O_2.
- j Refers to dissolving mineral species, *i.e.* UO_2 and pyrite.
- w Refers to the water-based leaching fluid.

Superscripts

- 0 Refers to the initial amount.
- ° Refers to standard system.
- d Refers to the dissolution reaction.

ACKNOWLEDGMENTS

The authors would like to thank Pennsylvania State University faculty members A. C. Lasaga and T. Ertekin for their valuable advice during the course of this research. Helpful discussions with M. McKibben, K. J. Breen, and B. Takano are also acknowledged. Research was supported by the United States Bureau of Mines Contract No. J0100065 to L. M. Cathles and H. L. Barnes, by the NSF, Geochemistry Program Grant No. EAR-8206777 to H. L. Barnes, and by the Ore Deposits Research and Mineral Conservation Sections, College of Earth and Mineral Sciences, The Pennsylvania State University. This research comprised the major portion of the senior author's doctoral dissertation.

REFERENCES

1. D. Langmuir: *Geochim. Cosmo. Acta*, 1978, vol. 42, pp. 1547-69.
2. P. Galichon, R. S. Schecter, A. Cowley, and M. Breland: *In Situ*, 1977, vol. 2, pp. 125-46.
3. P. S. Sundar: U.S. Bur. Mines Final Rep. 140-77, Dept. of the Interior, Washington, DC, 1977.
4. D. C. Grant: U.S. Bur. Mines Open File Rep. 52-79, Dept. of the Interior, Washington, DC, 1979.
5. T. A. Tatom: M. S. Dissertation, Chemical Engineering Dept., University of Texas, Austin, TX, 1981.
6. J. B. Goddard and D. R. Brosnahan: *Min. Eng.*, 1982, vol. 34, pp. 1589-96.
7. L. E. Eary and L. M. Cathles: *Metall. Trans. B*, 1983, vol. 14B, pp. 325-34.
8. A. R. Amell and D. Langmuir: U.S. Bur. Mines Final Rep., Contract No. H0272019, Dept. of the Interior, Washington, DC, 1978.
9. Y. Hekim and H. S. Fogler: *Am. Inst. Chem. Eng.*, 1980, vol. 26, pp. 403-11.
10. R. L. Rimstidt and H. L. Barnes: *Geochim. Cosmo. Acta*, 1980, vol. 44, pp. 1683-99.
11. L. E. Eary: Ph.D. Dissertation, The Pennsylvania State University, University Park, PA, 1983.
12. C. L. Wiersma and R. L. Rimstidt: *Geochim. Cosmo. Acta*, 1984, vol. 48, pp. 85-92.
13. P. C. Singer and W. Stumm: Federal Water Quality Rep. 14010-06/69, Contract PH36-66-107, Dept. of the Interior, Washington, DC, 1970.
14. M. A. McKibben: Ph.D. Dissertation, The Pennsylvania State University, University Park, PA, 1984.
15. D. K. Nordstrom: *Acid Sulfate Weathering*, Soil Science Soc. America, Madison, WI, 1982, pp. 37-62.
16. F. Gronvold: *J. Inorg. Nucl. Chem.*, 1955, vol. 1, pp. 355-70.
17. M. M. Jones, J. S. MacDuff, and A. B. Whitehead: U.S. Bur. Rep. Invest. 8433, Dept. of the Interior, Washington, DC, 1980.
18. H. Tamura, K. Goto, T. Yotsoyonagi, and M. Nagagama: *Talanta*, 1974, vol. 21, pp. 314-18.
19. G. D. Christian: *Analytical Chemistry*, Xerox College Publishing, Waltham, MA, 1971, pp. 327-28.
20. G. M. Eisenburg: *Ind. Eng. Chem., Anal. Ed.*, 1943, vol. 15, pp. 327-28.
21. A. C. Lasaga: *Kinetics of Geochemical Processes, Reviews in Mineralogy*, A. C. Lasaga and R. J. Kirkpatrick, eds., Mineralogical Society of America, Washington, DC, 1981, vol. 8, pp. 1-67.
22. L. E. Eary: *Metall. Trans. B*, 1985, vol. 16B, pp. 181-86.
23. T. F. Tsui: *Soc. Petr. Eng. J.*, Oct. 1984, pp. 563-74.